BBA - Gene Regulatory Mechanisms 1861 (2018) 473–480

Contents lists available at ScienceDirect

BBA - Gene Regulatory Mechanisms

journal homepage: www.elsevier.com/locate/bbagrm

Modulation of the endocrine transcriptional program by targeting histone modifiers of the H3K27me3 mark

Marta Fontcuberta-PiSunyer[a,b], Sara Cervantes[a,c], Eulàlia Miquel[d], Sergio Mora-Castilla[e], Louise C. Laurent[e], Angel Raya[d,f,g], Ramon Gomis[a,b,c,h], Rosa Gasa[a,c,*]

[a] Diabetes and Obesity Research Laboratory, August Pi i Sunyer Biomedical Research Institute (IDIBAPS), Rosselló 149-153, 08036 Barcelona, Spain
[b] University of Barcelona, Barcelona, Spain
[c] Centro de Investigación Biomédica en Red de Diabetes y Enfermedades Metabólicas Asociadas (CIBERDEM), Spain
[d] Center of Regenerative Medicine in Barcelona (CMRB), Hospital Duran i Reynals, Hospitalet del Llobregat, Barcelona, Spain
[e] Department of Reproductive Medicine, University of California, San Diego, La Jolla 92093, CA, USA
[f] Center for Networked Biomedical Research on Bioengineering, Biomaterials and Nanomedicine (CIBER-BBN), Spain
[g] Institució Catalana de Recerca i Estudis Avançats (ICREA), Barcelona, Spain
[h] Department of Endocrinology and Nutrition, Hospital Clinic of Barcelona, Barcelona, Spain

A B S T R A C T

Posttranscriptional modifications of histones constitute an epigenetic mechanism that is closely linked to both gene silencing and activation events. Trimethylation of Histone3 at lysine 27 (H3K27me3) is a repressive mark that associates with developmental gene regulation during differentiation programs. In the developing pancreas, expression of the transcription factor Neurogenin3 in multipotent progenitors initiates endocrine differentiation that culminates in the generation of all pancreatic islet cell lineages, including insulin-producing beta cells. Previously, we showed that Neurogenin3 promoted the removal of H3K27me3 marks at target gene promoters *in vitro*, suggesting a functional connection between this factor and regulators of this chromatin mark. In the present study, we aimed to specifically evaluate whether targeting the activity of these histone modifiers can be used to modulate pancreatic endocrine differentiation. Our data show that chemical inhibition of the H3K27me3 demethylases Jmjd3/Utx blunts Neurogenin3-dependent gene activation *in vitro*. Conversely, inhibition of the H3K27me3 methyltransferase Ezh2 enhances both the transactivation ability of Neurogenin3 in cultured cells and the formation of insulin-producing cells during directed differentiation from pluripotent cells. These results can help improve current protocols aimed at generating insulin-producing cells for beta cell replacement therapy in diabetes.

1. Introduction

Diabetes mellitus is characterized by absolute or relative insulin deficiency, which leads to hyperglycemia. The central role of insulin-producing pancreatic β-cells in the pathogenesis of diabetes makes this disease an ideal candidate for the application of regenerative medicine approaches. The generation of replacement β-cells from pluripotent stem cells through stepwise directed differentiation protocols, or from fully-differentiated somatic cells through direct reprogramming strategies are contemplated as promising developments with great potential in therapeutical applications for diabetes.

Site-specific covalent modification of histones constitutes a chromatin remodeling mechanism that plays a crucial role in the activation of cell-specific transcriptional programs during development. Trimethylation of histone3 at lysine 27 (H3K27me3) is a histone mark that is associated with transcriptional repression of a subset of genes that classically encode for developmental regulators. In embryonic stem cells, many developmental genes are concomitantly enriched in trimethylation at H3K27 and H3K4 (an active mark), creating a bivalent state in which genes are poised for activation but remain inactive until the repressive mark is removed. In the pancreas, H3K27me3 enrichment patterns dynamically change in the course of formation of β-cells from progenitors [2]. Remarkably, inadequate changes in H3K27me3 modification patterns have been associated with impaired endocrine gene activation during *in vitro* differentiation, which may partly underlie the immaturity of the β-cells generated *ex vivo* following these protocols [3].

Ezh2, a component of the Polycomb Repressive complex 2 (PRC2) is

* Corresponding author at: Diabetes and Obesity Research Laboratory, August Pi i Sunyer Biomedical Research Institute (IDIBAPS), Rosselló 149-153, 08036 Barcelona, Spain.
E-mail address: rgasa@clinic.cat (R. Gasa).

https://doi.org/10.1016/j.bbagrm.2018.03.003
Received 21 September 2017; Received in revised form 6 March 2018; Accepted 7 March 2018
Available online 09 March 2018
1874-9399/

a methyltransferase for H3K27me3. Conditional deletion of the *Ezh2* gene in mice has revealed that Ezh2 restrains the formation of pancreatic progenitors from endoderm [4] and of endocrine progenitors from pancreatic progenitors [5]. Conversely, H3K27me3 marks are removed by the Jumonji domain-containing demethylases Jmjd3 (Kdm6b) and Utx (Kdm6a) [6]. Knockdown of Jmjd3 in directed differentiation protocols from stem cells has been shown to result in abnormal definite endodermal formation [3]. Particular roles of these demethylases in the formation of pancreatic endocrine cells are unknown.

The generation of endocrine progenitors during pancreatic development entails expression of the transcription factor Neurogenin3 (NEUROG3) that functions as a transcriptional activator of the endocrine program. We previously showed that ectopic expression of NEUROG3 in cultured cells promotes loss of H3K27me3 marks at the proximal promoters of key downstream target genes [7], pointing to the engagement of this transcription factor with chromatin modulators of H3K27me3. In the current study, we have aimed at investigating the role of H3K27me3 marks in the initiation of endocrine differentiation by NEUROG3. We show that the activity of H3K27me3 demethylases is required for NEUROG3-dependent gene transactivation and that pharmacological manipulation of H3K27me3 levels can be used to modulate NEUROG3 activity *in vitro*. Additionally, we show that by blocking the action of H3K27me3 methyltransferases we can enhance insulin expression during directed endocrine differentiation from iPSCs. These results support the idea that the use of small molecule modulators of chromatin-modifying enzymes may serve to improve transcription factor (TF) based-cellular direct reprogramming protocols for generation of surrogate β-cells.

2. Materials and methods

2.1. Cell culture and viral transfection

Mouse pancreatic cells mPAC L20 were cultured in Dulbecco's modified Eagle's medium (DMEM) supplemented with 10% (v/v) fetal bovine serum and antibiotics. Mouse Embryonic Fibroblasts (MEFs) were isolated from prenatal mouse embryos between day E12.5-E14.5 following previously established protocols (https://ki.mit.edu/sbc/escell/methods/isolating with modifications). MEFs were maintained in high-glucose DMEM supplied with 10% (v/v) FCS, 2 mM L-glutamine (Gibco) and antibiotics. The human induced pluripotent stem cell line FiPS-4F-7 was obtained from the National Stem Cell Bank (BNLC) and maintained on Corning [8] Matrigel (BD) in mTeSR1 media (StemCell Technologies). Medium was changed every other day. The chemical inhibitors used were: EI-1 (Millipore), GSK-126 (Active Biochemicals) and GSK-J4 (Tocris Bioscience). They were added to the culture medium after viral transduction unless otherwise stated.

For adenoviral treatment, cells were seeded onto 6-well plates (Western blot and gene expression analyses) or 10 cm dishes (ChIP) one day before adenoviral treatment. At 70–80% confluence, cells were incubated with adenoviruses encoding NEUROG3, HA-Neurog3 or B-galactosidase at a multiplicity of infection (MOI) of 40 for 2–3 h at 37 °C in complete culture medium. Then, virus-containing medium was replaced and cells were maintained in culture for 48 h unless otherwise stated. Production of the recombinant adenoviruses was described previously [9,10].

2.2. Directed differentiation protocol

Pancreatic differentiation was induced in FiPS-4F-7 cells following a previously described protocol [11] with some modifications. Epigenetic inhibitors were added during the time intervals indicated in the Results section.

2.3. Western blot

For histone immunoblots, proteins were obtained by acid extraction in lysis buffer containing 0.2 N HCl. For determination of transgene expression, whole cell extracts were prepared with triple detergent lysis buffer (TrisHCl pH 8 50 mM, NaCl 150 mM, SDS 0.1%, Igepal CA-630 1%, Na deoxycholate 0.5%). Proteins (25 μg) were separated in a 16%Tris-Tricine (histones) or 12% Tris-Glycine (whole extracts) PAGE-SDS gel, transferred to PVDF membranes and incubated overnight at 4 °C with rabbit anti-mouse H3K27me3 (Abcam,1:500), rabbit anti-mouse Histone3 (H3) (Abcam,1:1000), mouse anti-HA (Sigma, 1:1000) and mouse anti-αTubulin (Sigma, 1:1000). Bands were visualized with ECL (Termo Scientific). Band quantification was performed using software Image Studio Lite (Li-COR, Biosciences).

2.4. RNA isolation and reverse transcriptase polymerase chain reaction (RT-PCR)

Total RNA was isolated using the High pure RNA Isolation Kit (Roche) following the manufacturer's manual. First-strand cDNA was prepared using Superscript III Reverse Transcriptase (Invitrogen) and random hexamers in a total volume of 20 μl. 1/40 to 1/200 of the resulting cDNA was used as a template for real time PCR reactions. Real time PCR was performed on an ABI Prism 7900 detection system using Gotaq master mix (Promega). Expression relative to a housekeeping gene was calculated using the deltaCt method. The primer sequences and amplicon lengths are provided in Supplementary Table S1.

2.5. Quantitative chromatin immunoprecipitation (ChIP) assay

Cells were fixed with 1% formaldehyde for 7 min and cross-linking was quenched by addition of 0.125 mM glycine. Cell pellets were lysed in SDS buffer (EDTA 10 mM, Tris.HCl 50 mM pH 8.1, SDS 1%). Chromatin was sheared between 0.3–0.5 kb by sonication and then cleared by centrifugation and diluted 1:10 in buffer containing 0,01% SDS, 1,1% triton X-100, 1.2 mM EDTA, 16.7 mM Tris-HCl pH 8.1, 16.7 mM NaCl. Antibody binding was carried overnight at 4 °C using a 2.5 μg of anti-H3K27me3 (Millipore), anti-H3K4me3 (Millipore), anti-H3K27ac (Abcam) or normal rabbit IgG as control (Sigma). Protein G magnetic beads (Millipore) were used to precipitate the antibody-bound complexes. Immunoprecipitates were washed and were eluted from the beads in 50 mM NaHCO3 containing 1% SDS, crosslinking was reversed by incubation at 62 °C for 3 h and DNA was purified using Qiaquik columns (Qiagen) and eluted in water. Immunoprecipitated DNA was assayed by real time PCR. Primers used are listed in Supplementary Table S1.

2.6. Statistical analysis

Data are presented as mean ± standard error of the mean (S.E.M). Statistical significance was tested using Student's *t*-test for independent samples and indicated in the figure legends.

3. Results

3.1. Temporal correlation between NEUROG3-induced transcriptional activation and changes in histone marks

Introduction of NEUROG3 induces the endocrine transcriptional program in mPAC cells [9]. We previously showed that gene activation in response to NEUROG3 correlated with loss of repressive H3K27me3 marks on the activated genes [7]. Here we have studied the temporal correlation between these two processes using as example a subset of genes known to be directly bound by NEUROG3 [7,10,12,13]. As shown in Fig. 1A–B, loss of H3K27me3 marks and increased transcript levels of *Atoh8* and *Insm1*, which display a bivalent (enriched in both H3K27me3

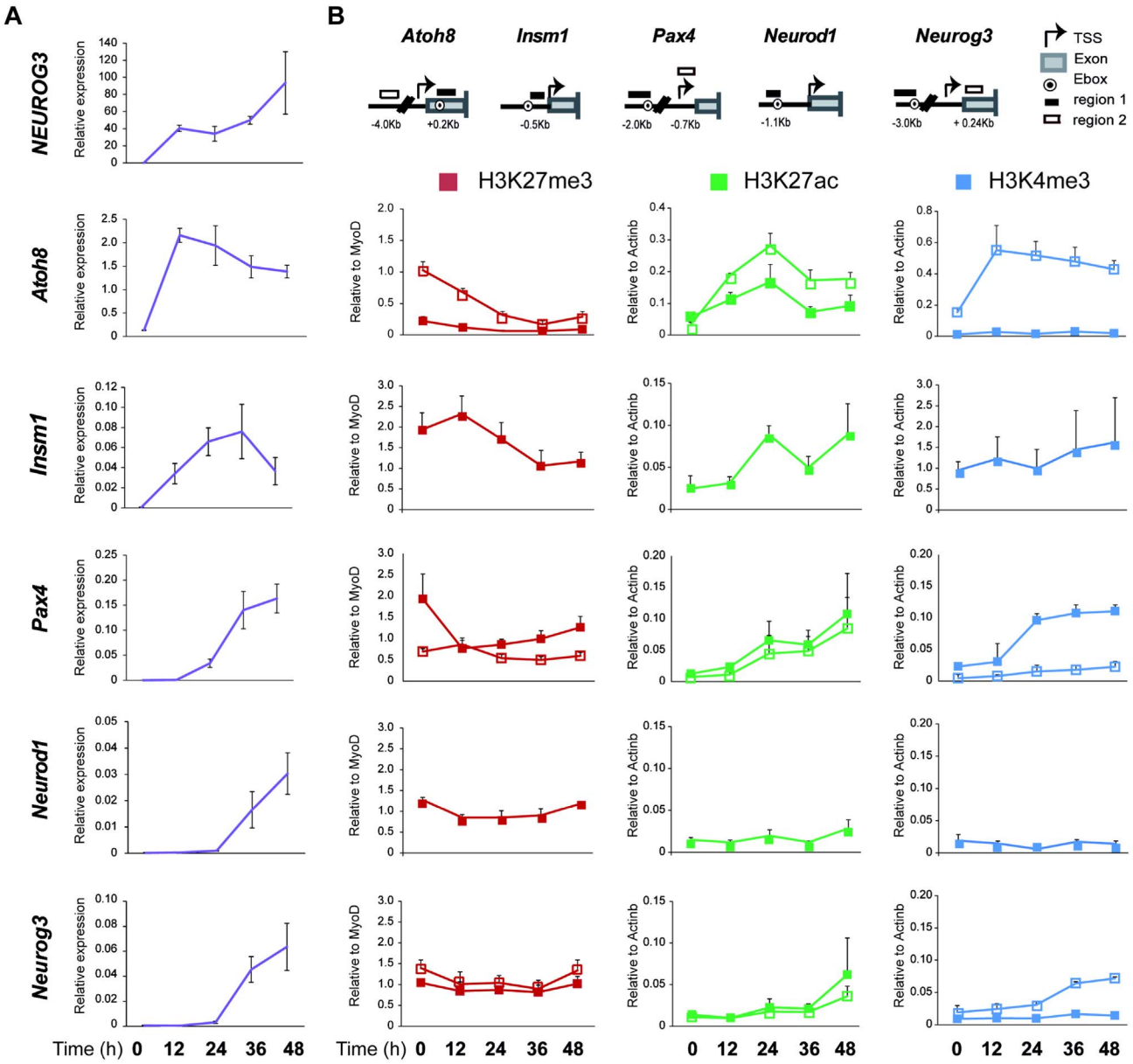

Fig. 1. Time-dependent changes in H3K27me3, H3K27ac and H3K4me3 enrichments and mRNA levels upon NEUROG3 expression in mPAC cells. mPAC cells were treated with a recombinant adenovirus encoding NEUROG3 and cultured for 48 h. (A) Total RNA was extracted and transcript levels for the transgene and the indicated endogenous genes were determined by real time PCR and expressed relative to *Tbp*. Results represent mean ± SE for 4 independent experiments (B) Chromatin was immunoprecipitated with tri-methylated H3K27 (H3K27me3), acetylated H3K27 (H3K27ac) and tri-methylated H3K4 (H3K4me3) specific antibodies and associated DNA was analyzed by real time PCR. Regions amplified are depicted as segments in gene diagram. Filled squares correspond to regions where target E box is located (region 1). Enrichment was calculated relative to MyoD (H3K27me3) or Actinb (H3K27ac and H3K4me3) at each time point. ChIP results are mean ± SE for 4–6 independent experiments.

and H3K4me3) status, were observed within 24 h of the transduction with the adenovirus, 12 h after detection of *NEUROG3* transgene expression. Seemingly, early responsive non-bivalent *Pax4* exhibited rapid loss of this mark at the upstream region containing the NEUROG3-binding site. By contrast, late targets *NeuroD1* and *Neurog3* showed almost no change in H3K27me3 during the 48 h period studied (Fig. 1A–B). Because these values represent an average over a cell population, within which not all cells are equally responsive to NEUROG3 [9,10], the high basal H3K27me3 levels at these promoters might have hindered the detection of decreases of this mark in a fraction of cells. To overcome this limitation, we studied H3K27 acetylation (H3K27ac), an antagonistic mark of H3K27me3, which is associated with active transcription and thus not found in these promoters in control (no NEUROG3) cells. With the exception of *Neurod1*, all genes exhibited deposition of H3K27ac (Fig. 1B). Likewise, H3K4me3 was deposited in close correlation with changes in H3K27 marks and transcriptional activation of these genes (Fig. 1B). Together, these data support the temporal association between removal of H3K27me3 marks and transactivation events elicited by NEUROG3.

3.2. Chemical inhibition of H3K27 demethylases Jmjd3 and Utx blocks NEUROG3-induced gene activation

Next, we asked whether loss of H3K27me3 was required for transcriptional activation of NEUROG3 target genes. The H3K27me3 demethylases Jmjd3 and Utx are both expressed endogenously in mPAC cells and their transcript levels are not modified upon NEUROG3 expression, thus indicating that changes in their expression are not responsible for changes in H3K27me3 levels in response to NEUROG3 (Fig. 2A). To evaluate the role of Jmjd3/Utx activity in NEUROG3

function we used a chemical inhibitor of both demethylases, GSK-J4. Treatment with GSK-J4 caused a small increase in total cellular levels of H3K27me3 (Fig. 2B), without significant changes in basal H3K27me3 enrichment at specific promoters (Fig. 2C). Nonetheless, GSK-J4 inhibited NEUROG3 gene transactivation events, which correlated with decreased H3K27ac deposition at target promoter sequences (Fig. S1). By contrast, expression of *Sox9*, which is endogenously expressed and not targeted by NEUROG3, was not changed (Fig. 2D). Further, reduced NEUROG3 activity in the presence of GSK-J4 was not due to decreased transgene expression levels as shown by immunoblot analysis (Fig. S2). Together, these results reveal that NEUROG3 requires the activity of H3K27me3 demethylases to activate genes enriched in this repressive mark.

3.3. Chemical inhibition of Ezh2 improves NEUROG3 transactivation activity

Given our findings with GSK-J4 we hypothesized that inhibition of the methyltransferase Ezh2 might improve NEUROG3-dependent endocrine differentiation. mPAC cells endogenously express Ezh2 and, interestingly, introduction of NEUROG3 decreases *Ezh2* transcript levels in these cells (Fig. 3A). Incubation with the Ezh2 inhibitor El-1 reduced both cellular H3K27me3 levels and enrichment for this mark at specific promoters, which was accompanied by increased deposition of active H3K27ac (Fig. 3B–D). In the absence of NEUROG3, the switch in postranslational marks of H3K27 elicited by E1-1 had not impact on gene expression of silent genes, although it increased transcript levels of *Atoh8*, which is already transcribed under control (no NEUROG3) conditions. In contrast, upon NEUROG3 introduction, addition of EI-1 resulted in an additional increment in H3K27ac deposition at target promoters (Fig. S1), which was accompanied by higher NEUROG3-induced gene transactivation of these genes (Fig. 3E–F). The potentiation of NEUROG3-induced gene activation elicited by EI-1 was not related to transgene expression changes as revealed by immunoblot analysis (Fig. S2). Lastly, enhancement of NEUROG3 action was validated with another Ezh2 inhibitor, GSK-126 (Fig. S3).

We then examined the temporal requirements for the potentiatory effects of Ezh2 inhibition and found that addition of the inhibitor prior to introduction of NEUROG3 had deleterious effects in the activation of most of the NEUROG3 target genes studied except *Atoh8* (Fig. 4). Therefore, Ezh2 inhibition and NEUROG3 activity need to occur simultaneously to have a positive impact on the transactivation ability of this transcription factor. Overall, these results support the idea that inhibition of Ezh2 could help boost the activity of NEUROG3 in cellular reprogramming protocols.

In view of the prior results we decided to examine whether Ezh2 inhibition could enhance the gene transactivation ability of NEUROG3 in less receptive cellular contexts; for instance, in distant cell lineages such as mouse embryonic fibroblasts (MEF). We found that NEUROG3 alone was able to induce expression of several endocrine genes in

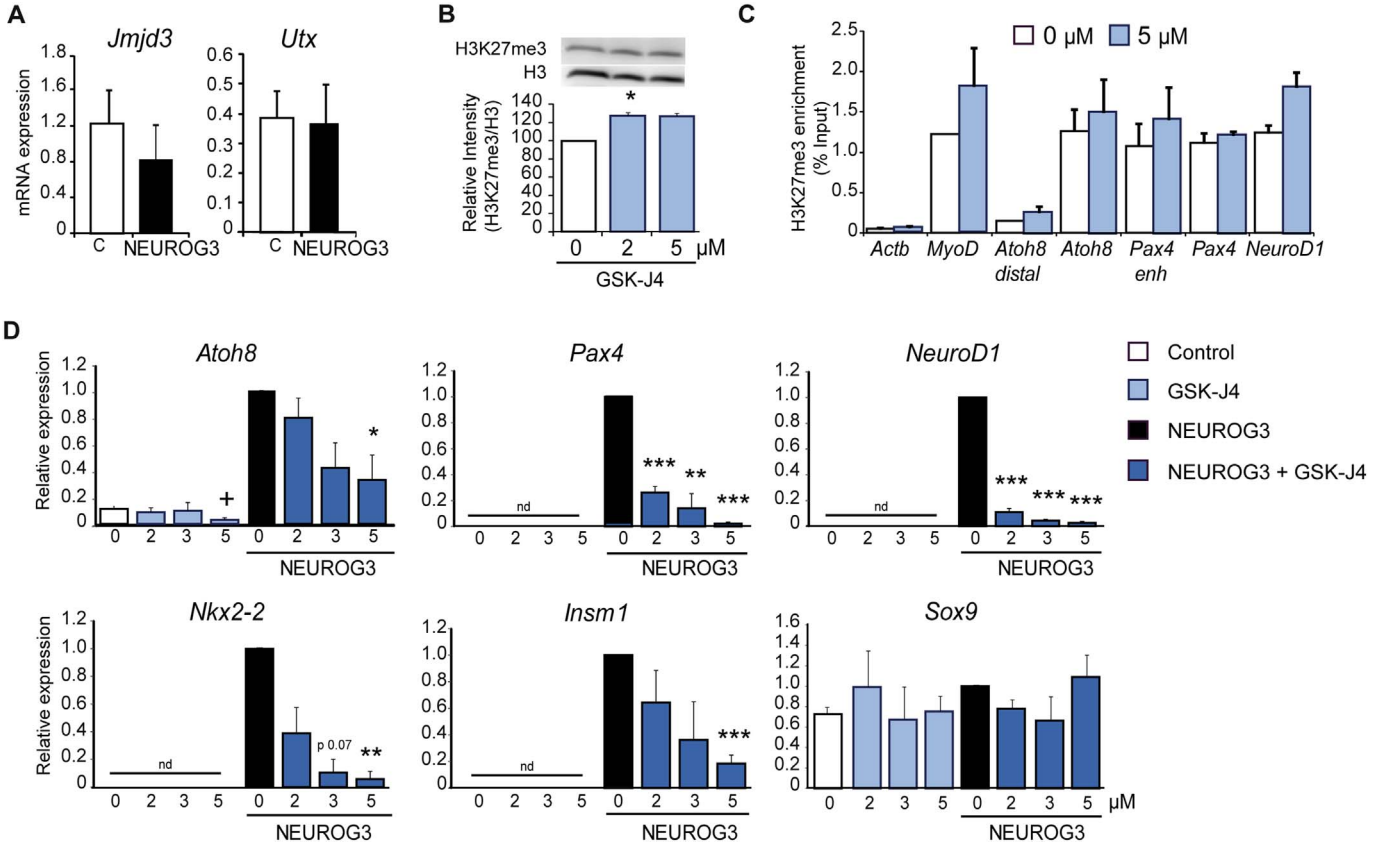

Fig. 2. Effects of chemical inhibition of the H3K27me3 demethylases Jmjd3/Utx in the transactivation ability of NEUROG3 in mPAC cells (A) mPAC cells were transduced with an adenovirus encoding NEUROG3 and collected 48 h after viral treatment. Gene expression levels of *Jmjd3* and *Utx* were studied by qPCR and are shown relative to *Tbp*. Data are mean ± SE for 3–4 independent experiments. (B–D) mPAC cells were treated with the indicated concentrations of GSKJ4 for 48 h. (B) Total H3K27me3 levels were determined by immunoblot analysis. Data are mean ± SE for 3 independent experiments; *p < 0.05 relative to cells cultured without inhibitor. (C) H3K27me3 enrichment at specific promoters was studied by ChIP. Proximal promoters of the *Actinb* and *MyoD* genes were included as control for non-target constitutively active and inactive gene, respectively. Data are mean ± SE from 4 independent experiments *p < 0.05, **p < 0.01, ***p < 0.001 relative to control. (D) mPAC cells were transduced with an adenovirus encoding NEUROG3 and cultured for 48 h in the presence of the indicated concentrations of GSKJ4. Total RNA was extracted and gene expression was evaluated by qPCR. Values are expressed relative to mRNA levels in cells treated with the NEUROG3-encoding adenovirus without inhibitor (value of 1). *Sox9* is expressed in mPAC cells and is not a NEUROG3 target. Of the NEUROG3 gene targets studied, only *Atoh8* is endogenously expressed in mPAC cells (nd: non detectable). Data is mean ± SE for 4–5 independent experiments. $^{+}$p < 0.05 relative to control; *p < 0.05, **p < 0.01, ***, p < 0.001 relative to NEUROG3 without inhibitor (black bar).

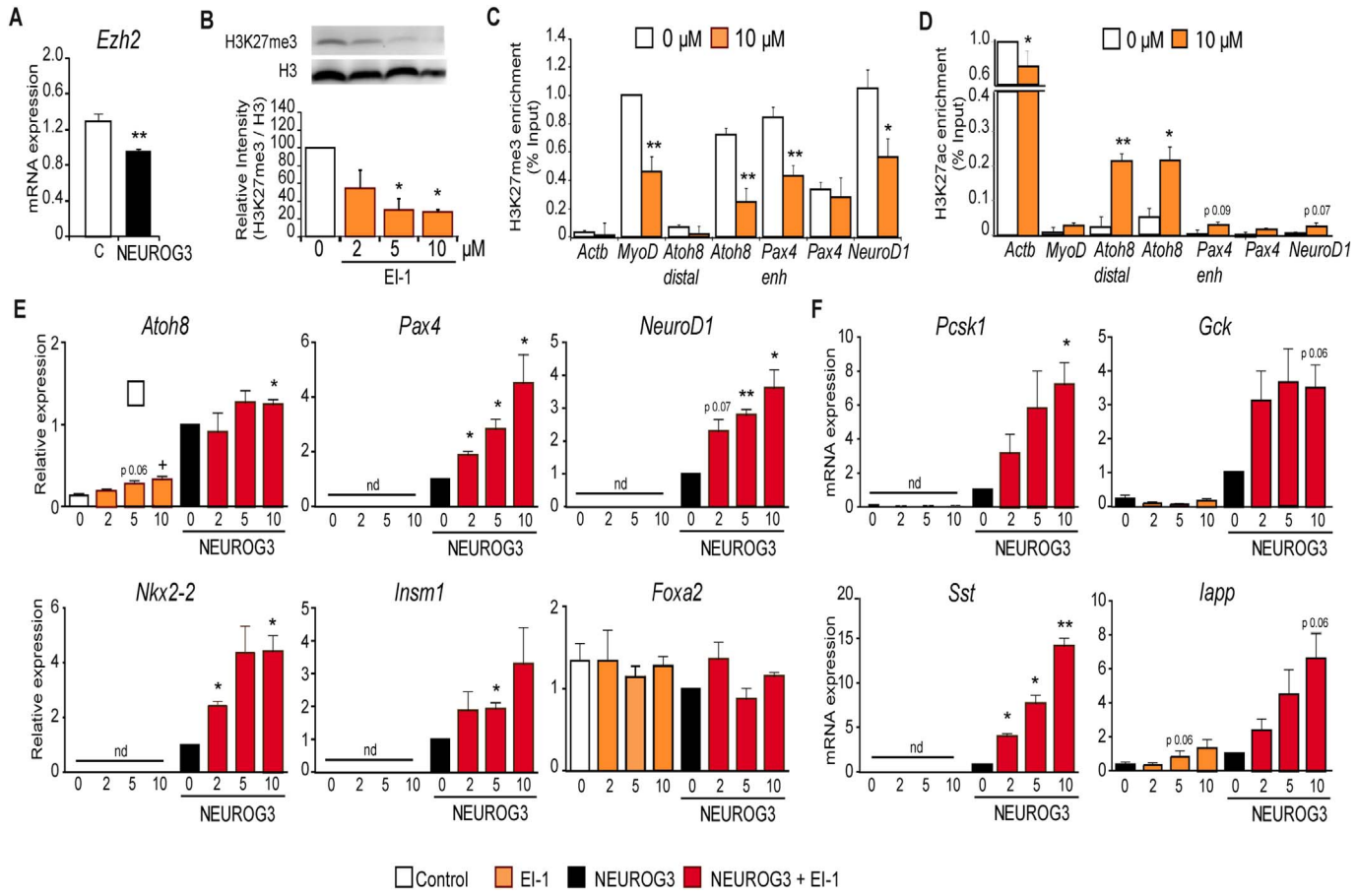

Fig. 3. Effects of chemical inhibition of the H3K27me3 methylase Ezh2 in the transactivation ability of NEUROG3 in mPAC cells (A) mPAC cells were transduced with an adenovirus encoding NEUROG3 and collected 48 h after viral treatment. Gene expression levels of *Ezh2* were studied by qPCR and are shown relative to *Tbp*. Data are mean ± SE for 4 independent experiments; **p < 0.01 (B–D) mPAC cells were treated with the indicated concentrations of EI-1 for 48 h. (B) Total H3K27me3 levels were determined by immunoblot analysis. Data are mean ± SE for 3 independent experiments; *p < 0.05 relative to cells cultured without inhibitor. (C) H3K27me3 and (D) H3K27ac enrichment at specific promoters was studied by ChIP. Associated DNA was analyzed by qPCR. Proximal promoters of the *Actinb* and *MyoD* genes were included as control for non-target constitutively active and inactive genes, respectively. Data are mean ± SE from 4 independent experiments *p < 0.05, **p < 0.01, ***p < 0.001 relative to cells not treated with the inhibitor. (E–F) mPAC cells were transduced with an adenovirus encoding NEUROG3 and cultured for an additional 48 h in the presence of EI-1 at the indicated concentrations. Total RNA was extracted and gene expression was evaluated by qPCR. Values are expressed relative to mRNA levels in cells treated with the NEUROG3-encoding adenovirus without inhibitor (value of 1). Foxa2 is endogenously expressed and is not a NEUROG3 target. (nd: non detectable). Data are mean ± SE for 4–5 independent experiments. $^{+}$p < 0.05 relative to control; *p < 0.05, **p < 0.01, ***p < 0.001 relative to NEUROG3 without inhibitor (black bar).

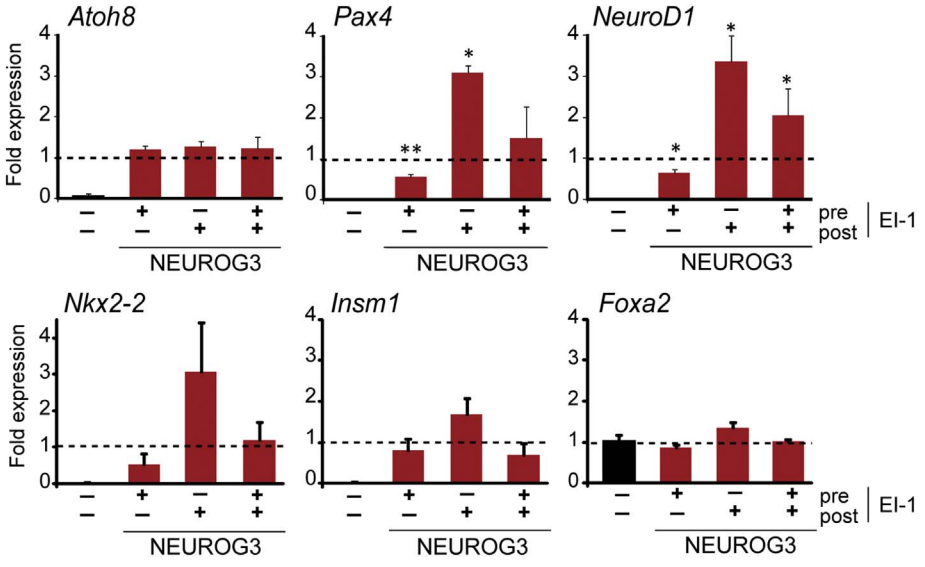

Fig. 4. Effects of time of addition of the Ezh2 inhibitor in the transactivation ability of NEUROG3 in mPAC cells. mPAC cells were cultured in the presence of 10 μM EI-1 for 24 h before adenoviral treatment (pre) or cultured in the presence of 10 μM EI-1 for 48 h after viral treatment [1], or both. Then, total RNA was extracted and gene expression was studied by qPCR. Values are expressed as fold relative to mRNA levels in cells treated with the NEUROG3-encoding adenovirus without inhibitor (value of 1 and represented by the broken line). Data are mean ± SE for 3–4 independent experiments. *p < 0.05, **p < 0.01, ***p < 0.001 relative to NEUROG3 without inhibitor.

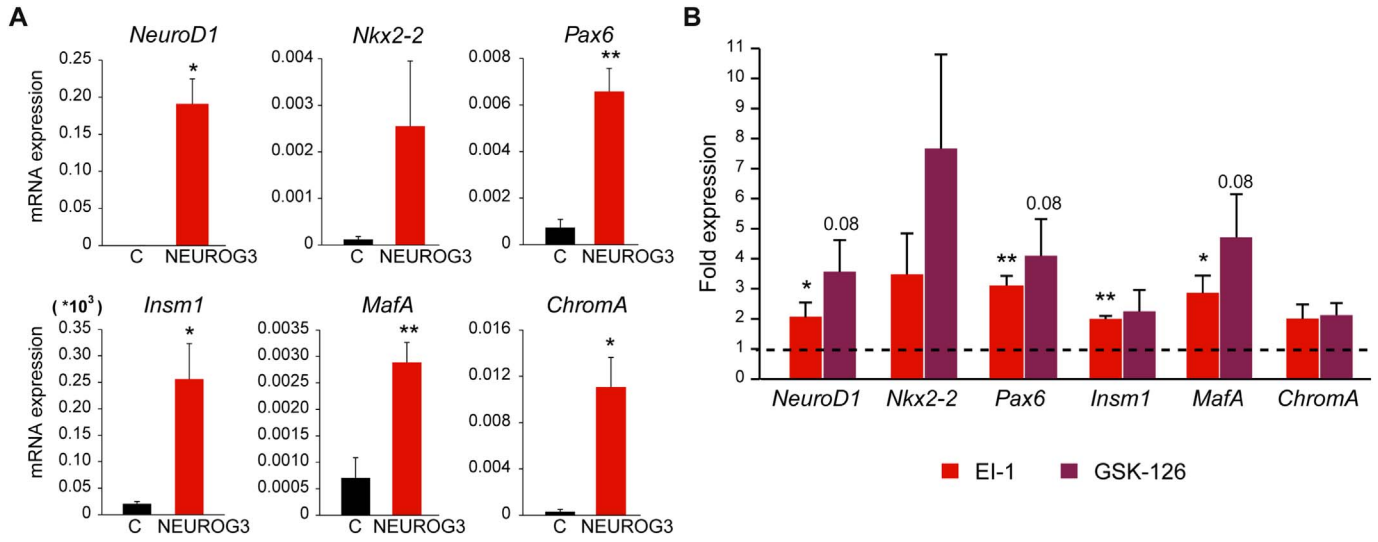

Fig. 5. Effects of chemical inhibition of Ezh2 in the transactivation ability of NEUROG3 in MEFs. Mouse embryonic fibroblasts were transduced with the NEUROG3-encoding adenovirus and cultured for additional 48 h after viral treatment in the presence of 10 μM EI-1 or 10 μM GSK126. Total RNA was extracted and gene expression was studied by qPCR (A) Gene expression of Neurog3 gene targets in untreated MEFs (C) or NEUROG3-expressing MEFs. Levels are expressed relative to *Tbp*. (B) Effects of the Ezh2 inhibitors on the indicated genes. Values represent fold-expression relative to mRNA levels in cells treated with the NEUROG3-encoding adenovirus without inhibitor (value of 1 and represented by the broken line). Data are mean ± SE for 4 independent experiments. *$p < 0.05$; **$p < 0.01$ relative to controls MEFs (A) or NEUROG3 without inhibitor (B).

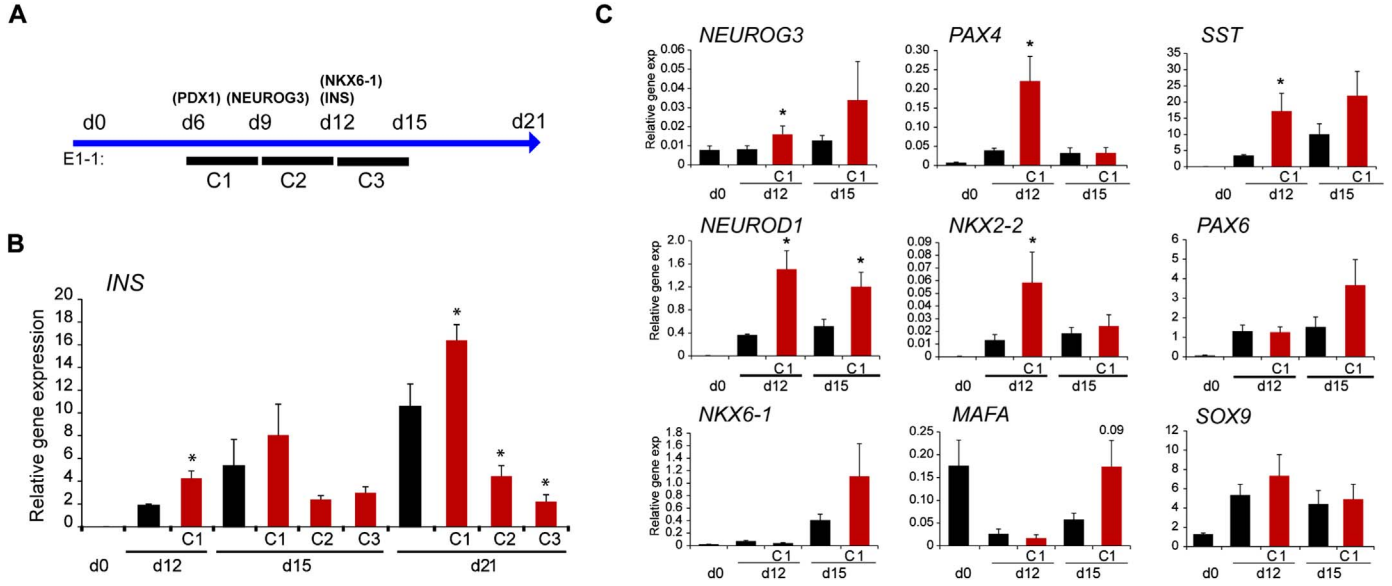

Fig. 6. Effects of EZH2 inhibition in the directed differentiation of human iPSC towards islet cells. (A) Experimental scheme of the 21-day directed differentiation protocol showing the times of EI-1 (20 μM) treatment (bars named C1, C2 and C3). In parenthesis, genes whose transcripts are first detected at the indicated day (B–C). Cells were collected and the indicated days of the protocol. Total RNA was extracted and transcript levels for the indicated genes were quantified by qPCR and expressed relative to *TBP*. Black bars indicate gene expression levels in control cells not treated with the inhibitor. Data are mean ± SE for 2–3 independent differentiation experiments, each in duplicate or triplicate. *$p < 0.05$ relative to control cells collected the same day of the protocol (black bars).

fibroblasts (Fig. 5A). Furthermore, concomitant inhibition of Ezh2 resulted in significant higher mRNA levels for some of the genes including *NeuroD1*, *Pax6*, *Nkx2.2* and *MafA* (Fig. 5B). All together, these results suggest that the use of chemical inhibitors of Ezh2 may be advantageous in transcription factor-based reprogramming protocols towards endocrine/β-cells.

3.4. Effects of chemical inhibition of Ezh2 in directed differentiation of pluripotent cells towards beta cells

The positive results obtained in transcription factor-based transdifferentiation experiments prompted us to test the effect of inhibiting Ezh2 in directed differentiation protocols using pluripotent cells. Chemical inhibition of Ezh2 has been shown to increase formation of insulin-producing cells by promoting *NEUROG3* expression in a human endodermal differentiation system *in vitro* [5]. Here we aimed at assessing if Ezh2 inhibition enhanced β-cell formation from human iPSC using a directed differentiation protocol. To determine the timing of endocrine differentiation following our protocol and better select when to add the inhibitor, we initially assessed the temporal expression profile of *NEUROG3* mRNA and found that it peaked at day 9, declined by day 12 and modestly increased again at day 21 (Fig. S4). On the other hand, *PDX1*, an early pancreas specification marker, was first detected at day 6 and both the β-cell genes *INS* and *NKX6.1* were initially detected at day 12 and increased prominently by day 21 (Fig. S4). Based on these findings, we added EI-1 on days 6–9 (birth of

endocrine progenitors) and on days 9–12 or 12–15 (during active endocrine differentiation) as depicted in Fig. 6A. RNA was collected at days 0, 12, 15 and 21 and gene expression was analyzed by qRT-PCR. As shown in Fig. 6B, treatment of EI-1 during days 6–9 (C1) resulted in higher *INS* gene expression at the end of the protocol, which is in agreement with previous findings [5]. Immunostaining and counting of INS+ cells demonstrated that the higher levels of *INS* gene expression corresponded to increased numbers of insulin-expressing cells (Fig. S5). On the contrary, inhibition of EZH2 at later stages during active endocrine cell genesis (C2 and C3) resulted in significantly lower *INS* transcript levels as compared to cells following the standard protocol (Fig. 6B). Based on these results, we focused on the C1 condition to examine the status of the endocrine transcriptional program. At day 12, several genes were found significantly upregulated as compared to control cells including *NEUROG3*, *PAX4*, *NEUROD1*, *SST* and *NKX2-2* (Fig. 6C), which would be compatible with enhanced NEUROG3 activity as all of these genes are known NEUROG3 targets [9]. Interestingly, another set of genes including *PAX6*, *NKX6-1* and *MAFA*, which are expressed in developing and differentiated β-cells, remained similar at day 12 whilst they tended to be more expressed at day 15 relative to control cells. By contrast, expression of SOX9 was unchanged in the C1 condition at either day 12 or 15. Taken together, these results demonstrate that inhibition of EZH2 activity prior to the peak of *NEUROG3* expression (day 9 in our protocol) can be used to enhance the endocrine transcriptional program and positively influence the number of insulin-expressing cells generated in directed differentiation protocols using pluripotent cells.

4. Discussion

The chromatin conformation is known to influence gene expression and, when in a “non-permissive” compact state, can represent a barrier for successful cell reprogramming. Here, we aimed at assessing if manipulation of the activity of chromatin-modifying enzymes might be a useful strategy to enhance TF-based and directed endocrine differentiation protocols. Specifically, we have studied the impact of chemically-modulating the activity of H3K27me3 regulators on the transactivation ability of NEUROG3. NEUROG3 is the key transcription factor that initiates the endocrine transcriptional cascade in pancreatic progenitors during embryogenesis [14]. Further, NEUROG3, alone or in combination with other TFs, has been used as a cell reprogramming factor to promote endocrine differentiation in several cellular contexts both *in vivo* and *in vitro* [9,15–19].

Dosage and activity of H3K27me3 demethylases have been correlated with the ability of several TFs to regulate gene expression programs [20]. We initially proposed the involvement of H3K27me3 in NEUROG3-dependent transactivation events based on our findings that forced expression of this factor promoted release of H3K27me3 marks at target promoter regions [7], but loss of H3K27me3 could either be a consequence or precede transcriptional activation of these genes [23,24]. Here we show that inhibition of H3K27me3 demethylases impairs the ability of NEUROG3 to transactivate genes. Whether it is Utx, Jmjd3, or both, that are involved in this effect cannot be disclosed from our data as GSK-J4 and other available chemical compounds inhibit both demethylases. Furthermore, it is conceivable that the specific demethylase involved may vary depending on the cellular context in which NEUROG3 is introduced.

As opposed to the H3K27me3 demethylase inhibitor, chemical inhibition of Ezh2 resulted in enhanced NEUROG3-dependent gene expression. Previous reports had implicated Ezh2 in restricting the progression from pancreatic to endocrine progenitors through negative regulation of the *Neurog3* gene [5]. Our present findings reveal that manipulation of Ezh2 activity can also be used to influence the function of NEUROG3. It is interesting that ectopic NEUROG3 decreases *Ezh2* gene expression in mPAC cells, an observation that relates with findings from our group showing that, *in vivo*, *Ezh2* gene expression is reduced in pancreatic endocrine progenitors compared to non-endocrine pancreatic cells [25]. Despite the known relevance of H3K27me3 marks in the regulation of developmental genes, it has been reported that changes in gene expression are not always associated with widespread changes in H3K27me3 deposition [26]. In this line, it is noteworthy that induction of the late target *Neurod1* in response to NEUROG3 occurred without detectable changes in H3K27me3 enrichment at the *Neurod1* promoter in mPAC cells. Despite this, *Neurod1* induction was drastically suppressed by the Jmjd3/Utx inhibitor and enhanced by the Ezh2 inhibitor. Thus, we cannot rule out that these effects are secondary to changes in the expression of intermediary gene/s that are required for NEUROG3-triggered *Neurod1* gene induction.

In general, most chromatin-modifying enzymes are expressed ubiquitously and specific gene expression patterns are thought to be mediated by their interaction with lineage specific factors in a context-dependent manner [21,22]. In this regard, it should be noted that our attempts to demonstrate physical association between adenovirally-expressed NEUROG3 and endogenous Jmjd3/Utx or Ezh2 using co-immunoprecipitation with commercially-available antibodies have been unsuccessful (data not shown). Nonetheless, the observation that changes in histone marks occur in the same gene regions where E boxes bound by NEUROG3 are located [7,10,12,13] indirectly supports that these chromatin modifiers and NEUROG3 are neighbors.

In addition to NEUROG3-mediated transdifferentiation, we show that inhibition of EZH2 is also effective in promoting endocrine differentiation in directed differentiation protocols using human iPSC. Importantly, the timing of exposure to the chemical inhibitor of EZH2 is critical to influence *INS* gene activation either positively or negatively in this system. The mechanistic reason for this observation is unclear. The stage between days 6 and 9 coincides with drastic induction of the *NEUROG3* gene and hence with birth of NEUROG3+ cells. We speculate that these early-born endocrine progenitors that express high levels of NEUROG3 will be most responsive to EZH2 inhibition in terms of NEUROG3 transactivation ability. In support of enhanced activation of the endocrine program, transcript levels for genes activated downstream of NEUROG3 were found increased at days 12 and/or 15 in cells treated with the inhibitor during days 6–9. In contrast, inhibition of EZH2 after day 9, when *NEUROG3* transcripts and thus NEUROG3 activity are decaying, is detrimental to endocrine differentiation. One possibility is that inhibition of EZH2 in late endocrine progenitors or differentiating endocrine cells might interfere with silencing of specific sets of genes [2] and hamper correct establishment of the endocrine program. Similar to our present findings, Xu et al. showed that inhibition of EZH2 during endocrine specification, but not earlier during pancreatic progenitor formation, resulted in a higher percentage of insulin positive cells in a human endodermal progenitor differentiation system *in vitro* [5]. Therefore, the time window for maneuver of H3K27me3 levels and improvement of endocrine differentiation appears to be limited to the stage during which NEUROG3+ cells are born. Future studies should be conducted to establish the functionality of the insulin-producing cells generated using this epigenetic manipulation.

To date, several examples of successful direct reprograming towards beta cells have been reported using developmentally close cell types, including pancreatic ductal, pancreatic exocrine, intestinal, hepatic or stomach cells [9,15–19]. Simultaneous use of chromatin-modifying agents and TF has been reported to improve endocrine gene activation in response to endocrine reprogramming transcription factors [27]. However, for potential medical applications, somatic cell reprogramming protocols should use readily accessible tissue such as skin. Fibroblasts have been successfully converted into different lineages including neurons, cardiomyocytes or hepatocytes using specific sets of TFs, but they appear to be poorly susceptible to TF-based transdifferentiation towards β-cells [19,27,28]. Here we show that introduction of NEUROG3 in MEFs can induce expression of endocrine differentiation genes but not of genes encoding the islet hormones, and that

concomitant inhibition of Ezh2 enhances the trans-activation ability of this TF. Epigenetic agents that broadly affect DNA methylation or histone acetylation were reported to induce expression of endocrine genes from dermal fibroblasts [28]. By contrast, our results show that inhibition of Ezh2 alone does not promote induction of silent endocrine genes in the absence of NEUROG3, either in MEFs or in mPAC cells. This difference may be explained by the more restricted enrichment pattern of the H3K27me3 mark as compared to the broader presence of acetylated histones at gene promoters. However, it is also possible that combining inhibition of a ubiquitous chromatin regulator together with a differentiation transcription factor provides some gene-specificity to the former.

In summary, this study demonstrates that manipulation of the repressive mark H3K27me3 can be used to influence the transactivation ability of NEUROG3 in cell-based assays and in directed differentiation protocols from pluripotent cells. These results are encouraging and support the idea that targeting specific chromatin modifiers may be a valid tactic to improve the transdifferentiation ability of β-cell reprogramming factors.

Supplementary data to this article can be found online at https://doi.org/10.1016/j.bbagrm.2018.03.003.

Transparency document

The Transparency document associated this article can be found, in online version.

Acknowledgments

We are indebted to Lidia Sanchez and Yaiza Esteban for excellent technical assistance, and to Mercè Martí for help with the study design of IPS experiments. This work has been supported by project 120230 (to RGa) from Fundació Marató de TV3, PI13/01500 and PI16/00774 (to RGa) integrated in the Plan Estatal de I+D+I and cofinanced by ISCIII-Subdirección General de Evaluación and Fondo Europeo de Desarrollo Regional (FEDER-"A way to build Europe"), and grant 2014 SGR659 (to RGo) from the Generalitat de Catalunya. The research leading to these results has received funding from the European Community's Seventh Framework Programme (FP7/2009-2013) under the grant agreement n°229673 (SC); ISCIII/FEDER (FIS PI14/01682; Red de Terapia Celular - TerCel RD16/0011/0024), Generalitat de Catalunya-AGAUR (2014-SGR-1460), and CERCA Programme/Generalitat de Catalunya. CIBERDEM (Centro de Investigación Biomédica en Red de Diabetes y Enfermedades Metabólicas Asociadas) is an initiative of the Instituto de Salud Carlos III. MF has been funded by Generalitat de Catalunya (2014 SGR659).

Author contributions

Conceived and designed the experiments: MF, RGa. Performed the experiments: MF, SC, EM Analyzed the data: MF, RGa. Discussed the data: MF, SC, RGo, RGa, SM, LC, AR. Wrote the manuscript: MF, RGa.

References

[1] C. Postic, M. Shiota, K.D. Niswender, T.L. Jetton, Y. Chen, J.M. Moates, et al., Dual roles for glucokinase in glucose homeostasis as determined by liver and pancreatic beta cell-specific gene knock-outs using Cre recombinase, J. Biol. Chem. 274 (1) (1999) 305–315.

[2] J. van Arensbergen, J. Garcia-Hurtado, I. Moran, M.A. Maestro, X. Xu, M. Van de Casteele, et al., Derepression of Polycomb targets during pancreatic organogenesis allows insulin-producing beta-cells to adopt a neural gene activity program, Genome Res. 20 (6) (2010) 722–732.

[3] R. Xie, L.J. Everett, H.W. Lim, N.A. Patel, J. Schug, E. Kroon, et al., Dynamic chromatin remodeling mediated by polycomb proteins orchestrates pancreatic differentiation of human embryonic stem cells, Cell Stem Cell 12 (2) (2013) 224–237.

[4] C.R. Xu, P.A. Cole, D.J. Meyers, J. Kormish, S. Dent, K.S. Zaret, Chromatin "pre-pattern" and histone modifiers in a fate choice for liver and pancreas, Science 332 (6032) (2011) 963–966.

[5] C.R. Xu, L.C. Li, G. Donahue, L. Ying, Y.W. Zhang, P. Gadue, et al., Dynamics of genomic H3K27me3 domains and role of EZH2 during pancreatic endocrine specification, EMBO J. 33 (19) (2014) 2157–2170.

[6] M.R. Hubner, D.L. Spector, Role of H3K27 demethylases Jmjd3 and UTX in transcriptional regulation, Cold Spring Harb. Symp. Quant. Biol. 75 (2010) 43–49.

[7] G. Pujadas, F. Felipe, M. Ejarque, L. Sanchez, S. Cervantes, F.C. Lynn, et al., Sequence and epigenetic determinants in the regulation of the Math6 gene by Neurogenin3, Differentiation 82 (2) (2011) 66–76.

[8] G. Pujadas, S. Cervantes, A. Tutusaus, M. Ejarque, L. Sanchez, A. Garcia, et al., Wnt9a deficiency discloses a repressive role of Tcf7l2 on endocrine differentiation in the embryonic pancreas, Sci. Rep. 6 (2016) 19223.

[9] R. Gasa, C. Mrejen, F.C. Lynn, P. Skewes-Cox, L. Sanchez, K.Y. Yang, et al., Induction of pancreatic islet cell differentiation by the neurogenin-neuroD cascade, Differentiation 76 (4) (2008) 381–391.

[10] M. Ejarque, S. Cervantes, G. Pujadas, A. Tutusaus, L. Sanchez, R. Gasa, Neurogenin3 cooperates with Foxa2 to autoactivate its own expression, J. Biol. Chem. 288 (17) (2013) 11705–11717.

[11] C.H. Cho, N.R. Hannan, F.M. Docherty, H.M. Docherty, M. Joao Lima, M.W. Trotter, et al., Inhibition of activin/nodal signalling is necessary for pancreatic differentiation of human pluripotent stem cells, Diabetologia 55 (12) (2012) 3284–3295.

[12] G. Mellitzer, S. Bonne, R.F. Luco, M. Van De Casteele, N. Lenne-Samuel, P. Collombat, et al., IA1 is NGN3-dependent and essential for differentiation of the endocrine pancreas, EMBO J. 25 (6) (2006) 1344–1352.

[13] S.B. Smith, R. Gasa, H. Watada, J. Wang, S.C. Griffen, M.S. German, Neurogenin3 and hepatic nuclear factor 1 cooperate in activating pancreatic expression of Pax4, J. Biol. Chem. 278 (40) (2003) 38254–38259.

[14] G. Gu, J. Dubauskaite, D.A. Melton, Direct evidence for the pancreatic lineage: NGN3+ cells are islet progenitors and are distinct from duct progenitors, Development 129 (10) (2002) 2447–2457.

[15] C. Ariyachet, A. Tovaglieri, G. Xiang, J. Lu, M.S. Shah, C.A. Richmond, et al., Reprogrammed stomach tissue as a renewable source of functional beta cells for blood glucose regulation, Cell Stem Cell 18 (3) (2016) 410–421.

[16] Y.J. Chen, S.R. Finkbeiner, D. Weinblatt, M.J. Emmett, F. Tameire, M. Yousefi, et al., De novo formation of insulin-producing "neo-beta cell islets" from intestinal crypts, Cell Rep. 6 (6) (2014) 1046–1058.

[17] Y. Heremans, M. Van De Casteele, P. in't Veld, G. Gradwohl, P. Serup, O. Madsen, et al., Recapitulation of embryonic neuroendocrine differentiation in adult human pancreatic duct cells expressing neurogenin 3, J. Cell Biol. 159 (2) (2002) 303–312.

[18] V. Yechoor, V. Liu, C. Espiritu, A. Paul, K. Oka, H. Kojima, et al., Neurogenin3 is sufficient for transdetermination of hepatic progenitor cells into neo-islets in vivo but not transdifferentiation of hepatocytes, Dev. Cell 16 (3) (2009) 358–373.

[19] Q. Zhou, J. Brown, A. Kanarek, J. Rajagopal, D.A. Melton, In vivo reprogramming of adult pancreatic exocrine cells to beta-cells, Nature 455 (7213) (2008) 627–632.

[20] A. Benyoucef, C.G. Palii, C. Wang, C.J. Porter, A. Chu, F. Dai, et al., UTX inhibition as selective epigenetic therapy against TAL1-driven T-cell acute lymphoblastic leukemia, Genes Dev. 30 (5) (2016) 508–521.

[21] S. Seenundun, S. Rampalli, Q.C. Liu, A. Aziz, C. Palii, S. Hong, et al., UTX mediates demethylation of H3K27me3 at muscle-specific genes during myogenesis, EMBO J. 29 (8) (2010) 1401–1411.

[22] Y. Wang, Y. Li, C. Guo, Q. Lu, W. Wang, Z. Jia, et al., ISL1 and JMJD3 synergistically control cardiac differentiation of embryonic stem cells, Nucleic Acids Res. 44 (14) (2016) 6741–6755.

[23] M. Hosogane, R. Funayama, M. Shirota, K. Nakayama, Lack of transcription triggers H3K27me3 accumulation in the gene body, Cell Rep. 16 (3) (2016) 696–706.

[24] M. Hosogane, R. Funayama, Y. Nishida, T. Nagashima, K. Nakayama, Ras-induced changes in H3K27me3 occur after those in transcriptional activity, PLoS Genet. 9 (8) (2013) e1003698.

[25] S. Cervantes, M. Fontcuberta-PiSunyer, J.M. Servitja, R. Fernandez-Ruiz, A. Garcia, L. Sanchez, et al., Late-stage differentiation of embryonic pancreatic beta-cells requires Jarid2, Sci. Rep. 7 (1) (2017) 11643.

[26] J. Vanhove, M. Pistoni, M. Welters, K. Eggermont, V. Vanslembrouck, N. Helsen, et al., H3K27me3 does not orchestrate the expression of lineage-specific markers in hESC-derived hepatocytes in vitro, Stem Cell Rep. 7 (2) (2016) 192–206.

[27] E. Akinci, A. Banga, K. Tungatt, J. Segal, D. Eberhard, J.R. Dutton, et al., Reprogramming of various cell types to a beta-like state by Pdx1, Ngn3 and MafA, PLoS One 8 (11) (2013) e82424.

[28] L.S. Katz, E. Geras-Raaka, M.C. Gershengorn, Reprogramming adult human dermal fibroblasts to islet-like cells by epigenetic modification coupled to transcription factor modulation, Stem Cells Dev. 22 (18) (2013) 2551–2560.